

## ARTICLE

# Effect of temperature and moisture on the bond strength between fiber reinforced polymer laminates and cement-based mortar substrates

Peyman Imani Jajarmi<sup>1</sup> | Mohammadreza Tavakkolizadeh<sup>1</sup>  | Abbas Youssefi<sup>2</sup>

<sup>1</sup>Department of Civil Engineering,  
Ferdowsi University of Mashhad,  
Mashhad, Iran

<sup>2</sup>Par-e-Tavous Research Institute,  
Mashhad, Iran

## Correspondence

Mohammadreza Tavakkolizadeh,  
Department of Civil Engineering,  
Ferdowsi University of Mashhad, Azadi  
Square, Mashhad, Khorasan Razavi  
91775-1111, Iran.  
Email: drt@um.ac.ir

## Funding information

Ferdowsi University of Mashhad, Grant/  
Award Number: 52008

## Abstract

This paper presents the results of pull-off and twist-off tests on bond strength between fiber reinforced polymer (FRP) and cement-based mortar substrate and is carried out to investigate the effect of moisture and temperature at the time of installation. In the field of fracture mechanics, it is common to classify the pull-off and twist-off tests as mode-I and mode-II fractures, respectively. A total of 27 specimens were prepared and 243 tests were conducted. In order to evaluate the significance of each factor and their interactions, analysis of variance (ANOVA) was performed. Results revealed that surface moisture content and temperature significantly affect the adhesion of the two materials and bond strength. ANOVA confirmed that these two parameters have great influence on bond strength between FRP and cement-based mortar, although compressive strength and total porosity of substrate were not statistically significant. To estimate the bond strength by considering the effective parameters and based on the collected experimental data, new and more accurate relations were proposed using nonlinear regression techniques.

## KEYWORDS

bond strength, fiber-reinforced polymer, mortar substrate, moisture, pull-off, temperature, twist-off

## 1 | INTRODUCTION

There are many approaches to strengthen reinforced concrete (RC) beams and columns. One of the more effective methods is externally bonding fiber-reinforced polymer (FRP) laminates to the tension side of a beam or wrapping around a column using proper adhesive. The bond strength between FRP and cementitious substrates is

under the effects of mechanical, physical, and chemical conditions.

To avoid potential premature delamination from occurring, the following points should be considered:

- Proper environmental condition at the time of installation, such as relative humidity, surface moisture content, and temperature;
- sufficient surface preparation to obtain a rough, clean, and sound substrate;
- necessity of using primer, bonding agent or other inter-coat adhesives;
- preparing FRP laminates using appropriate fibers, resins, installation methods, and curing process.

Discussion on this paper must be submitted within two months of the print publication. The discussion will then be published in print, along with the authors' closure, if any, approximately nine months after the print publication.

Kanareh<sup>1</sup> recommended to ensure good performance and behavior of the FRP systems, and the concrete surface must be dry at the time of installation. Myers et al.<sup>2</sup> used pull-off, twist-off, and flexural tests to evaluate the effects of environmental conditions during installation of CFRP reinforcement. Test results revealed that maximum allowable surface moisture content and relative humidity were 4.3% and 82%, respectively. Also, they noted that FRP laminates could be installed within a temperature range of 4–49°C. However, some FRP manufacturers suggested the maximum allowable surface moisture content of 4% by volume.<sup>3</sup>

In order to investigate the effect of the moisture present on the surface of concrete before installation process, Wan et al.<sup>4</sup> studied interfacial energy release rate,  $G$ , of the CFRP–concrete bond. The test results indicated that adhesion between CFRP and concrete was significantly decreased when water was presented during primer application and curing. However, water-tolerant primer increased the bond strength of concrete substrates.

In a study by Dai et al.,<sup>5</sup> pull-off and bending tests were used to investigate the effects of moisture at the time of FRP installation and throughout the service life on the bond performance. Lu et al.<sup>6</sup> investigated the effect of moisture before installation and during service life on the bond strength between CFRP and concrete for three different types of epoxy resins. The bonding strength of FRP reinforcements to concrete exposed to three degrees of partial saturation (5%, 25%, and 50% humidity content) investigated by Cuomo et al.<sup>7</sup>

The objective of the studies of Pan et al.<sup>8,9</sup> and Shrestha et al.<sup>10</sup> was to examine the influence of water immersion on the bond between the CFRP and concrete. Water immersion causes significant degradation in the CFRP–concrete bond strength as interfacial fracture energy, shear, and tensile bond. The effect of the interface region relative humidity on the bond between CFRP and concrete was determined by Ouyang and Wan.<sup>11</sup> They also identified the moisture induced vapor and osmotic pressure in the interface can lead to local debonding in continuation of their research.<sup>12</sup>

Generally, migration of moisture molecules from concrete substrate to interface concrete-epoxy can affect the bond quality negatively during curing by creating a moisture barrier that prevents deep penetration of epoxy into irregularities and surface pores of concrete and improper curing of epoxy. Plasticization, hydrolysis, cracking, and crazing are reported as harmful effect of water molecules on the properties of epoxy resins.<sup>13</sup>

According to American concrete institute (ACI) committee 440 guidelines,<sup>14</sup> the maximum service temperature of an FRP strengthening system should be limited to  $T_g$  of the resin used. The  $T_g$ , glass transition temperature,

is the temperature at which epoxy transition from a rigid state to a viscoelastic state. Above the  $T_g$  value, properties of epoxy can be dramatically reduced and changes in molecular mobility, rigidity, volume, percent elongation to break may occur. A more conservative limit on maximum design temperature is recommended by American association of state highway and transportation officials (AASHTO) specifications,<sup>15</sup> where  $T_g$  is at least 22°C higher than the maximum design temperature. International federation for structural concrete (*fib*)<sup>16</sup> recommends that  $T_g$  of the adhesive used should be sufficiently large with respect to the service temperature and not less than 45°C.

According to Aiello et al.,<sup>17</sup>  $T_g$  must be at least 5–10°C above the expected service temperature. The effect of elevated service temperatures on the short- and long-term performance of adhesively bonded FRP reinforcement was investigated by Borchert and Zilch,<sup>18</sup> Luo and Wong,<sup>19</sup> Xian and Karbhari<sup>20</sup> and Ferrier et al.<sup>21</sup> The experimental results have shown that the FRP performance are sensitive to the condition temperature.

Nguyen et al.<sup>22</sup> investigations have shown that when the temperature exceeds the  $T_g$ , ultimate load capacity reduces significantly. Leone et al.<sup>23</sup> used double-lab shear test to determine the effect of elevated service temperature and showed a decrease of the maximum bond stress for service temperatures above the  $T_g$ , while maximum bond stress was obtained from specimens 50°C. The results are confirmed by Blontrock et al.<sup>24</sup> The effect of surface preparation and elevated temperature on CFRP–concrete bond strength was investigated by Attari and Tavakkolizadeh.<sup>25</sup> The effect of subzero temperature on the performance of FRPs has been investigated thoroughly by other researchers as well.<sup>26,27</sup>

In the present paper, the effect of environmental conditions during installation on the bond quality FRP systems was investigated. GFRP laminates were applied to 18 cement-based mortar specimens with six different surface temperatures, which lead to four different levels of working relative moisture. Additionally, GFRP laminates were applied to nine mortar substrates with three different relative moistures of 55%, 75%, and 95% at 25°C. The data obtained were statistically analyzed using analysis of variance (ANOVA). The correlation between the pull-off and twist-off strengths for different environmental conditions was obtained based on compressive strength and porosity of mortar substrate. New and more accurate relations were proposed using nonlinear regression techniques on data obtained from pull-off and twist-off tests for estimating bond strength of GFRP systems with different environmental conditions.

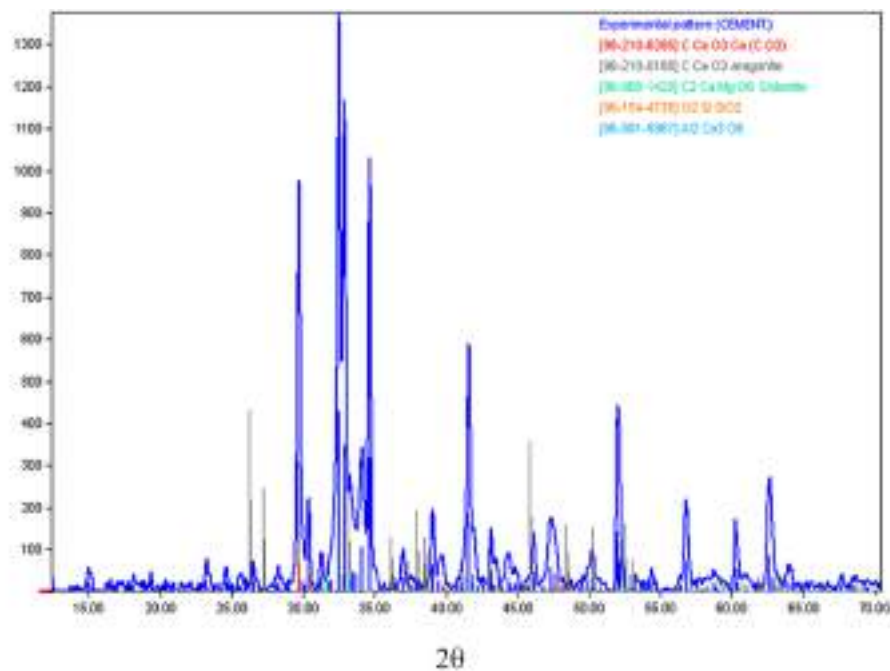
## 2 | EXPERIMENTAL WORKS

### 2.1 | Materials and specimen preparation

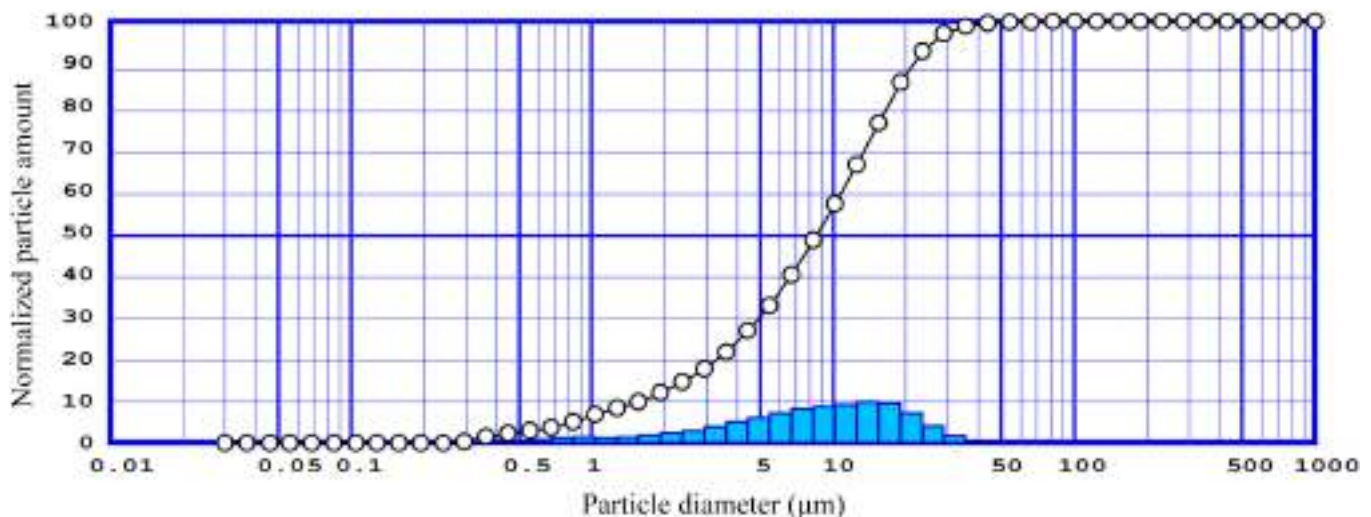
Cement-based mortar samples were prepared using Type I Portland cement and tested according to ASTM C109-20.<sup>28</sup> The average compressive strength of the cement paste was 17.33 and 41.57 MPa at 3 and 28 days, respectively. The X-ray diffraction (XRD) and particle

size distribution (PSD) of the cement composites are shown in Figure 1.

Fine aggregate PSD was done according to ASTM C144-18<sup>29</sup> and is shown in Figure 2. The sand has a fineness modulus of 3.81 and a maximum nominal size of 4.75 mm, which are within the grading limits specified by the ASTM standard. The specific gravity and absorption of the sand were determined in accordance with ASTM C128-15.<sup>30</sup> The specific gravity and absorption were 2.57% and 1.63%, respectively. The moisture content



(a)



(b)

FIGURE 1 Analysis of cement used in the study (a) XRD and (b) PSD

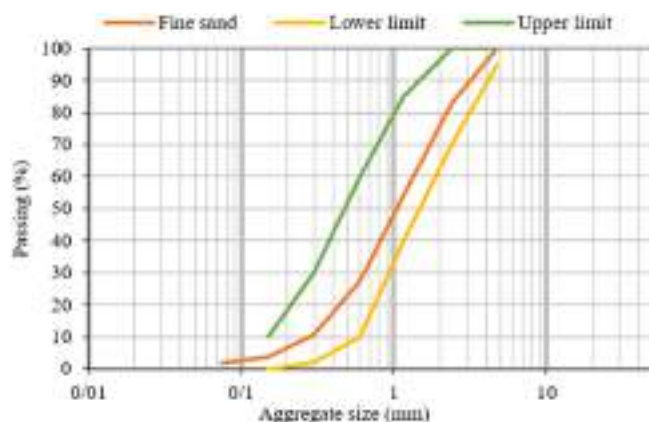


FIGURE 2 Gradation curve for fine aggregate compared with ASTM C144-18<sup>32</sup>

TABLE 1 Mortar mix proportions

Mortar mix	w/c	s/c	Cement (kg/m <sup>3</sup> )	Sand (kg/m <sup>3</sup> )	Water (kg/m <sup>3</sup> )
A	0.45	2.75	592.00	1628.00	266.4
B	0.55	2.75	559.00	1537.25	307.45
C	0.45	2.00	702.00	1404.00	315.90

of fine aggregates at the time of sample preparation was 6.91%.

In order to properly analyze the effect of properties, micro substructure, and porosity of the substrate on the bond strength FRP to concrete, two different water-cement ratios ( $w/c$ ) of 0.45 and 0.55 and sand-cement ratios ( $s/c$ ) of 2.75 and 2.00 were considered to prepare mortar specimens. Table 1 displays the mortar mix proportions used to cast the specimens. Since dry aggregates were used for the composition of mortars, the quantity of water needed to substitute the absorption capacity was added to the mix.

Fresh cement mortars were cast into well-oiled wooden molds to form  $150 \times 150 \times 50$  mm specimens. After 24 h at room temperature under moisture barrier, samples were demolded and submerged in a 25°C saturated lime water tank for 27 more days. Then bottom surfaces of specimens were dry sandblasted with 6 bar pressure from 150 mm distance with an average speed of 50 mm/s to expose the aggregate surfaces in order to remove cement paste layers and other impurities from the surface of the specimens.<sup>31–34</sup> One layer of unidirectional glass fabric was applied to the sandblasted surface using two-part epoxy resin (with amine type hardener). The  $T_g$  of the epoxy resin reported by the manufacturer was 45°C in normal curing temperature. The properties of the glass fabric and epoxy used in the study are presented in Table 2.

TABLE 2 Properties of glass fabric and epoxy resin used

Material	Tensile strength (MPa)	Elastic modulus (GPa)	Ultimate elongation (%)
Glass fabric	2200	70.0	3.0
Epoxy resin	55	2.5	2.6

## 2.2 | Environmental exposure

The bonding strengths of GFRP systems were investigated for two different conditions before FRP installation, namely:

- I. Different temperatures of the cementitious surface.
- II. Different moisture content of the cementitious surface.

GFRP laminates were installed on specimens from each mix that were kept at a temperature of 25°C with a surface moisture content of 35% (lab environment condition) as control specimens.

Mortar specimens for condition I were kept in a temperature control chamber (cooler or heater) for at least 5 days before the installation of GFRP laminates. The prescribed temperature conditions for these specimens were chosen as 5, 15, 25, 50, 80, and 120°C. The three higher temperatures of 50–120°C were chosen to investigate the effect of temperatures near and above  $T_g$ . The surface moisture content was measured at desired temperatures.

The mortar specimens for condition II first were submerged in freshwater for at least 5 days to be completely saturated. Then, they were removed from water and were allowed to gradually dry in laboratory environment at 25°C to reach the desirable surface moisture content for installation of GFRP laminates. A pin-type moisture meter was used to measure the moisture content of the specimen surface, based on the electrical resistance between two electrodes. Table 3 shows the moisture content and temperature of the specimens at the time of FRP installations.

## 2.3 | Compressive strength of mortar

The compressive strengths of the specimens were obtained according to ASTM C109-20<sup>28</sup> using 50 mm brass cube molds. Filled molds were covered and stored in laboratory for 24 h and then the specimens were removed from the molds and submerged in saturated lime water tank at room temperature for 27 more days.

Temperature (°C) and moisture content (%)

Condition A	5 and 50	15 and 46	25 and 35	50 and 0	80 and 0	120 and 0
Condition B	25 and 35	25 and 55	25 and 75	25 and 95	–	–

TABLE 3 Temperatures and moisture contents of specimens

For each batch, five compressive specimens were tested for each testing age of 3, 14, and 28 days and the average values reported.

## 2.4 | Flow of fresh mortar

Flow tests were performed according to ASTM C230-21<sup>35</sup> to evaluate the workability of the mortar mixes. A manual flow table with a diameter of 254 mm and a drop of 12.7 mm was used. The conical mold had dimensions of 101.6, 69.9, and 50.8 mm for bottom diameter, top diameter, and height, respectively.

## 2.5 | Water sorptivity and absorption of mortar

A variety of techniques have been developed to investigate the amount of water absorption for cementitious materials. The water absorption of a cement mortar depends on many factors including mix proportion, type of cement, type of fine aggregate, the type of curing, and the degree of hydration. Here, ASTM C1403-15<sup>36</sup> and ASTM C642-13<sup>37</sup> were used to measure water sorptivity and water absorption, respectively.

To measure water sorptivity, three 50 mm cubes were prepared for each batch of mortar mix. Samples were dried in an oven at a temperature of 110°C for not less than 24 hours. Before testing, the specimens were weighed and recorded as  $W_0$ . A part of the cube (about 3 mm) was immersed in water. The cube was removed at 0.25, 1, 4, and 24 hours and weighted as  $W_T$ . The water sorptivity is obtained using the following equation:

$$I = \frac{(W_T - W_0)}{L_1 \times L_2} \quad (1)$$

where  $L_1$  and  $L_2$  are the length and width of the test surface of the cube. Additionally, water absorption of mortar mixes at 0.5, 24, 48, and 72 h were measured by 100 mm cubes. Similar to the past test, samples were dried in an oven at a temperature of 110°C for not less than 24 h. After removing from the oven, cooling, and weighting, the samples were submerged in water for mentioned periods. In each time, cubes were removed from water

and manually dried with a paper towel and finally weighed. The water absorption is obtained using the following equation:

$$\text{Water absorption}(\%) = \frac{(W_T - W_0)}{W_0} \times 100 \quad (2)$$

where  $W_T$  and  $W_0$  are mass of surface-dried and oven-dried samples, respectively. The values of water sorptivity and absorption for the three mortar mixes were reported.

## 2.6 | Pull-off test

The pull-off test is a common and partially destructive technique used to assess the bond strength between two materials. The pull-off test is commonly employed for verifying in situ the resistance of the interface to mode-I fractures. The pull-off test produced a small area of damage compared with other destructive methods. Several standards prescribe the way the pull-off test should be performed.<sup>38–42</sup> In this study, ASTM D 7522-21<sup>39</sup> and ASTM D7234-19<sup>40</sup> were used to conduct the pull-off tests. The pull-off test is performed by gluing a test dolly to the surface of the FRP laminates with an adhesive. Before attaching the dollies, a partial coring was carried out through the FRP laminate on the surface of the mortar substrate using a core drill apparatus. The inner diameter of hole cutter should be the same the diameter as the dolly (Figure 3).

Note that the core had a depth of between 6 and 12 mm into the substrate. The center-to-center distances between consecutive dollies and to the edge of specimens should be at least two times of and equal to the diameter of the dolly, respectively. Italian national research council<sup>43</sup> suggested a minimum diameter of 25 mm for pull-off test. Additional recommendations on rate of loading, thickness of dolly, and number of bond tests are available in the literature.<sup>38–42</sup>

After the adhesive was cured, a testing apparatus was attached to the loading fixture and then exerted a tensile load perpendicular to the surface until either a plug of material was detached or a specified value was reached. The pull-off strength ( $f_p$ ) was calculated as the ratio of the pull-off force ( $F_p$ ) to the surface area of dolly using the following equation:



$$f_p = \frac{4F_p}{\pi D^2} \quad (3)$$

where  $D$  is the diameter of the dolly.

According to ASTM D7522-21,<sup>39</sup> different failure modes occur during the pull-off test, representing the weakest plan within the system. As shown in Figure 4, the six important types of failure modes to consider are as follows:

- A the failure at interface dolly and FRP;
- B cohesive failure in FRP;
- C adhesive failure at the interface between FRP and adhesive;
- E adhesive failure at the adhesive–concrete interface;

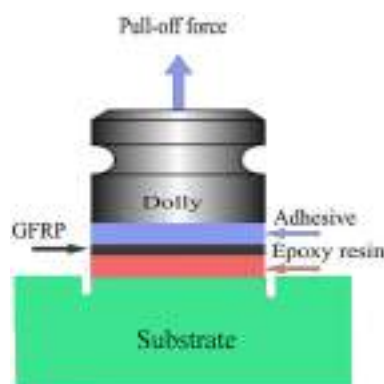


FIGURE 3 The assembly of pull-off test<sup>29</sup>

- G cohesive failure in the substrate;
- F mixed mode, including concrete and interface failure.

Failure mode A is not an acceptable failure mode, and failure mode G represents a complete bond between the repair materials and substrate. Pull-off test reliability depends on several factors such as the coring depth, geometry of dolly, rate of loading, possible loading of eccentricity, curing time, and thickness of the coating.<sup>44–48</sup>

Here, the pull-off tests as shown in Figure 5a were performed using the following steps:

- Select a flat surface of the substrate with proper distance from the edge and other cores.
- Scoring with a depth of 6 mm was performed through the GFRP down to the surface of the cement-based mortar substrate.
- Surface preparation of GFRP laminate and dolly to reach a perfect bonding to avoid mode A failure.
- A 22 mm diameter dolly was adhered to the surface of the GFRP laminate with an epoxy adhesive under constant contact pressure.
- Allow enough time for the adhesive to cure.
- The hydraulic jack and load cell were attached to the fixture and aligned so that tensile force was applied normal to the test surface without any eccentricity. Loading was applied at a constant rate of 0.05 MPa/s.

Five pull-off tests were conducted on each mortar specimen and the results were averaged and reported with the failure modes.

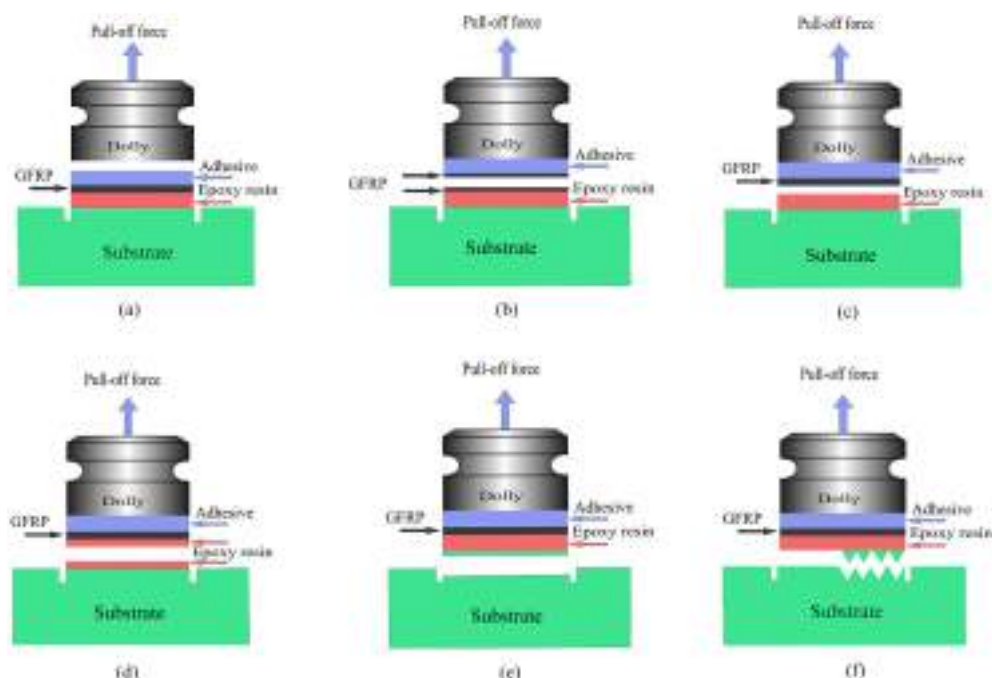


FIGURE 4 Types of failure modes: (a) failure mode A; (b) failure mode B; (c) failure mode C; (d) failure mode E; (e) failure mode G; and (f) failure mode F<sup>41</sup>



FIGURE 5 Test set up for bond test: (a) pull-off, (b) twist-off, and (c) location of the dolly for both tests

## 2.7 | Twist-off test

The twist-off test is another partially destructive method, which can be used in both in situ and laboratory to evaluate the bond strength between FRP laminates and concrete substrate. The method involves bonding a dolly to the surface of the FRP with an appropriate adhesive to avoid adhesive failure after applying proper coring. Next, the twist-off apparatus (calibrated torque meter) is attached to the dolly, and by exerting gradually increasing torque (without applying shear force), a plug of material is detached, and the greatest torque is recorded<sup>49</sup> which indicates mode-II fractures. The maximum applied shear stress can be used as twist-off strength of the bond. The torsional shear stress can be calculated using the following relation:

$$f_T = \frac{16T}{\pi D^3} \quad (4)$$

where  $D$  is the diameter of the dolly,  $T$  is the maximum applied torque, which is recorded by torque meter, and  $f_T$  is the twist-off strength.

Here, the twist-off tests as shown in Figure 5b were performed using the following steps:

- First five steps were similar to those that were described earlier.
- Torque meter was connected to the dolly and torque was applied without inserting additional shear force until the fixture separated from the surface. For mortar specimens, four twist-off tests were conducted and the results were averaged and reported.

Figure 5c shows the location of the dolly for pull-off and twist-off tests on a typical specimen.

## 3 | RESULTS AND DISCUSSIONS

### 3.1 | Compressive strength, modulus of elasticity, and total porosity of mixes

The values of compressive strength of mortar mixes at the age of 3, 7, and 28 days are presented in Table 4. It was observed that mortar with  $s/c$  of 2.75 and  $w/c$  of 0.45 (group A) exhibited the highest compressive strengths. At a given  $s/c$ , when  $w/c$  was increased, compressive strength decreased. It should be noted that increasing the  $w/c$  increases the number of water-filled spaces in the fresh cement mortar, which ultimately leads to a greater proportion of capillary pores in the hardened cement mortar specimens. In this case, permeability has been increased and compressive strength is decreased. The results demonstrated that the strength of hardened mortar depends on  $s/c$  when the  $w/c$  was kept constant. Group A had greater compressive strength than group C, which was in agreement with the previous reports that the optimal  $s/c$  was around 0.30–0.40.<sup>50</sup> As was expected, the compressive strength increased with time due to increase in the degree of hydration. The effect of  $w/c$  and  $s/c$  on the value of Young's modulus ( $E$ ) is also shown in Table 3. Group B displayed significantly lower values of  $E$  as a result of higher  $w/c$ .

The Virtual Cement and Concrete Testing Laboratory software (VCCTL), Version 9.5 was employed to evaluate the total porosities of cement-based mortars. The VCCTL package was developed at the National Institute of Standards and Technology,<sup>51</sup> to perform computations of various rheological, mechanical, and transport properties of cement-based materials such as 3D microstructure model, calibrate hydration kinetics, elastic moduli, compressive strength, heat release, chemical shrinkage, gel-space ratio and total porosities testing, and validation of the software

TABLE 4 Cement mortar material properties

Group	Compressive strength (MPa)			Young's modulus (GPa)	Flow (%)	Total porosity (%)
	3 (day)	7 (day)	28 (day)			
A	23.98	32.26	39.23	0.253	69.29	0.253
B	20.81	23.07	33.75	0.331	108.66	0.331
C	21.47	26.40	38.35	0.257	121.46	0.257

was done by various researchers in the past.<sup>52–55</sup> The results of calculated total porosity are shown in Table 4.

### 3.2 | The flow of fresh mortar

The results of the flow table tests on fresh cement-based mortar mixes are presented in Table 4. The amount of fresh mortar flow was determined by averaging four diameter measurements of fresh mortar spread on the flow table using a caliper. The results showed that the flow value increases proportionally as  $w/c$  increases, as reported by Chindaprasirt et al.<sup>50</sup> Additionally, at a given  $w/c$ , with the increase of cement content, workability of a mortar mix was increased.

### 3.3 | Water absorption of mortar

Figures 6 and 7 show average values of water sorptivity and water absorption for 50 and 100 mm cubes, respectively. According to Figure 6, the water sorptivity had a linear relationship with the square root of exposure time that is consistent with the results reported by other researchers.<sup>56</sup> As it is evident in Figure 7, absorption values become almost constant after 24 h of exposure to water. The observation indicates that the specimens with high  $w/c$  had a significantly greater content of capillary pore space, much of it interconnected, and thus had higher water permeability.

### 3.4 | Bond test

#### 3.4.1 | Failure modes

Four predominant failure modes were observed during bond tests:

- cohesive failure in mortar substrate (G);
- cohesive failure in FRP laminates (B);
- adhesive failure at the interface between FRP laminates and mortar substrate (E);

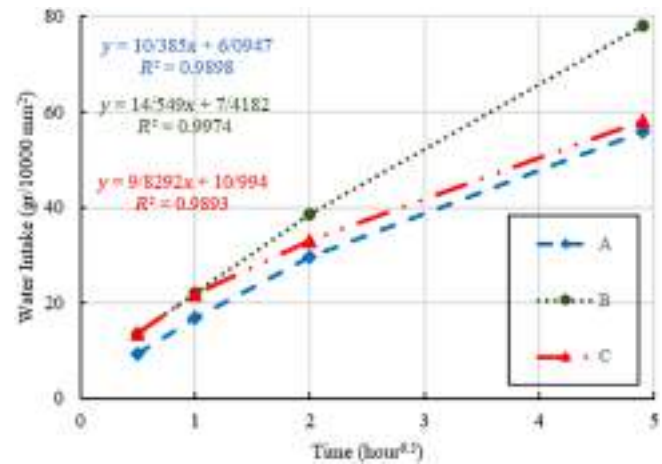


FIGURE 6 Sorptivity of mortar specimens by time

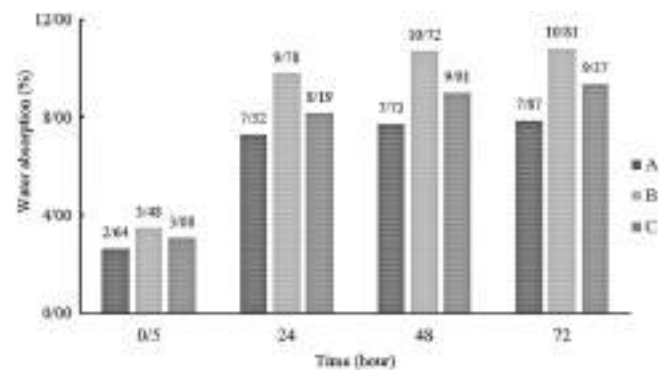


FIGURE 7 Water absorption of mortars

- mixed-mode failure including mortar failure and interface failure (F).

As shown in Figure 8, cohesive failure in mortar substrate (or in GFRP laminate) was a failure inside the mortar block substrate (or GFRP laminate), as shown in Figure 8a,b. Cohesive failure in the mortar substrate is the most desirable mode of failure and displays a remarkable performance of the retrofitting system. An adhesive failure occurred along the interface between the adhesive layer and the substrate and was due to inadequate chemical and mechanical bonds to the substrate as shown in





**FIGURE 8** Typical failure modes: (a) cohesive failure of mortar substrate; (b) cohesive failure of GFRP laminate; (c) mortar–adhesive interface failure and (d) mixed cohesive/adhesive failure

Figure 8c. Mixed cohesive/adhesive failure was a combination of cohesive and adhesive failure as shown in Figure 8d. This type of failure is expected to start cohesively in the substrate, and then propagate throughout the interface, becoming adhesive. Tables 5 and 6 present the failure modes of all tested specimens.

### 3.4.2 | Pull-off test

As reported in Table 5, for all of the specimens prepared at temperature below 25°C, the failure mode was interface and mixed. Specimens prepared at 25°C and above (up to 80°C) exhibited exceptional bond performance as the failure occurred in the mortar substrate. The tests indicated that with an increase of temperature from 80 to 120°C, the failure mode changed from cohesive failure in mortar to mixed mode and occasionally interface mode. This showed that the very high temperature of the substrate and subsequent curing environment had a negative effect on the bond between epoxy resin and mortar substrate. As shown in Figure 9, the light brown region represents the burned area of GFRP laminates exposed to high temperature.

For control specimens (installation at 25°C temperature and 35% surface moisture content), the failure mode was cohesive failure, regardless of the substrate characteristics. However, and in the contrast, with an increase of moisture content at mortar/adhesive interface, the failure mode changed from cohesive failure to mixed cohesive/adhesive failure and adhesive failure at the interface for 55% and 75% moisture content, respectively.

Specimens strengthened with a surface moisture content of 95% resulted in extremely poor bond behavior, so the dominant failure mode for groups A and C was interface failure. It should be noted that the GFRP laminates of the group B specimen installed at 95% moisture content were peeled off completely during coring operation or experienced interfacial failure without any significant load being applied to them, as shown in Figure 10. The trace of water particles present on the contact surface of the resin and the substrate and below the GFRP system was clear, as shown in Figure 10b.

The presence of water at the interface between mortar and adhesive decreases the bond strength of GFRP to mortar substrate because the hydrogen bonds between the epoxy and the substrate may be adversely affected by the presence of water molecules at the interface. In addition, water molecules have a negative impact on the mechanical interlocking as they could represent an obstacle to the penetration of epoxy into substrate surface pores.

The findings of previous studies have shown that interface failure mode indicates the weakening of the epoxy–concrete bond interface because of the moisture diffusion or the presence of defects within this region.<sup>57</sup> It is well understood that the presence of water and moisture content of the substrate during the installation process has an effect on the wettability and contact angle between adhesive and adherent.<sup>58</sup> Figure 11 describes the ratio of different failure modes obtained by pull-off test under the effect of temperature and surface moisture content.

TABLE 5 Effect of temperature on the pull-off, twist-off, and failure mode

Test group	Specimen #	Pull-off			Failure mode of pull-off	Mean ( $\bar{f}_p$ ) MPa	Standard deviation ( $\sigma$ ) MPa	Coefficient of variation (cv) %	Specimen #	Twist-off adhesion value ( $\bar{f}_T$ ) MPa	Failure mode of twist-off	Mean ( $\bar{f}_T$ ) MPa	Standard deviation ( $\sigma$ ) MPa	Coefficient of variation (cv) %
		adhesion value ( $\bar{f}_p$ ) MPa												
A-Control	1	4.99			Mortar	3.75	0.71	18.96	1	9.52	Mortar	9.88	0.55	5.61
	2	2.81			Mortar				2	10.84	Mortar			
	3	3.75			Mortar				3	9.64	Mortar			
	4	3.43			Mortar				4	9.53	Mortar			
	5	3.75			Mortar									
A-5	1	3.25			Interface	3.22	0.07	2.28	1	8.89	Mix	8.07	1.43	17.74
	2	3.34			Mix				2	5.65	Interface			
	3	3.12			Interface				3	9.31	Interface			
	4	3.18			Mix				4	8.42	Mix			
	5	3.21			Interface									
A-15	1	3.37			Mix	3.47	0.16	4.56	1	7.25	Mix	7.39	0.34	4.55
	2	3.75			Interface				2	6.91	Mix			
	3	3.28			Mix				3	7.77	Mix			
	4	3.50			Mix				4	7.63	Mix			
	5	3.46			Mortar									
A-50	1	4.43			Mortar	4.71	0.28	5.90	1	10.35	Mortar	10.87	0.46	4.20
	2	4.40			Mortar				2	11.58	Mortar			
	3	5.15			Mortar				3	10.63	Mortar			
	4	4.71			Mortar				4	10.92	Mortar			
	5	4.84			Mortar									
A-80	1	3.87			Mortar	3.81	0.12	3.28	1	7.87	Mortar	8.38	0.48	5.77
	2	3.93			Mortar				2	8.52	Mortar			
	3	3.59			Mortar				3	9.1	Mortar			
	4	3.90			Mortar				4	8.01	Mortar			
	5	3.75			Mortar									
A-120	1	3.25			Mix	3.27	0.09	2.66	1	5.27	Mix	6.32	1.00	15.84
	2	3.43			Mortar				2	7.88	Mix			
	3	3.21			Mortar				3	5.65	Mix			
	4	3.18			Mix				4	6.47	Mix			
	5	3.28			Mix									
B-Control	1	3.59			Mortar	3.53	0.06	1.66	1	9.28	Mortar	8.89	0.61	6.82
	2	3.53			Mortar				2	7.84	Mortar			
	3	3.59			Mortar				3	9.26	Mortar			
	4	3.43			Mortar				4	9.17	Mix			
	5	3.53			Mortar									

(Continues)









TABLE 6 (Continued)



**FIGURE 9** Failure mode at 120°C: (a) mixed cohesive/adhesive and (b) interface failure



**FIGURE 10** Failure modes of specimen installation at 95% moisture content: (a) interfacial failure without load-bearing capacity and (b) presence of water vapor on the interface

### 3.4.3 | Twist-off test

Similar to the pull-off test, different failure modes were observed for different specimens in different environment. For specimens that FRP installation performed at 5 and 15°C, the failure modes occurred as interface and mixed modes. The failure modes were changed to mortar cohesive failure with increasing installation temperature, except at 120°C. For half of the B-80 specimen, the failure mode was observed as a cohesive failure in GFRP laminates. In this temperature, the failure mode was cohesive failure in mortar.

For the control specimen at low moisture content, the failure was cohesive failure in mortar substrate, showing the integrity of the bond between GFRP laminates and mortar substrates. The failure mode was shifted from the cohesive failure to mixed cohesive/adhesive failure and interface debonding, as the moisture content increased to 55 and 75%, respectively. Also, for all of the specimens with 95% surface moisture content, interfacial failure mode was observed.

As mentioned earlier, these shifts in failure category are mainly due to moisture penetration into the epoxy-substrate interface and destruction of adhesion bonding. Percentages of the different failure modes observed in twist-off test can be seen in Figure 12.

## 3.5 | Bond strength

### 3.5.1 | Pull-off test

Tables 5 and 6 display the effects of surface temperature and moisture content on pull-off test strength for all the specimens and statistical parameters were calculated based on five tests on each mortar block. As results shows, these two parameters significantly affect the bond strength of FRP laminate to mortar substrate. For control specimens that GFRP installed at room environment (temperature of 25°C and moisture content of 35%), the pull-off strength of specimen groups A, B, and C were 3.75, 3.53, and 3.57 MPa, respectively.

Installation at 5°C temperature resulted in 14.04%, 15.62%, and 27.10% reduction in average bond strength for A, B, and C groups, respectively (Table 7). In contrast, an increase in the temperature leads to an increase in the values of the average bond strength between GFRP and mortar substrate. This phenomenon was due to the decrease in viscosity of adhesive and better penetration into pores of substrate as well as the increase in the cross-linking rate and the glass transition temperature of the epoxy resin during the increase of surface temperature.<sup>59,60</sup>

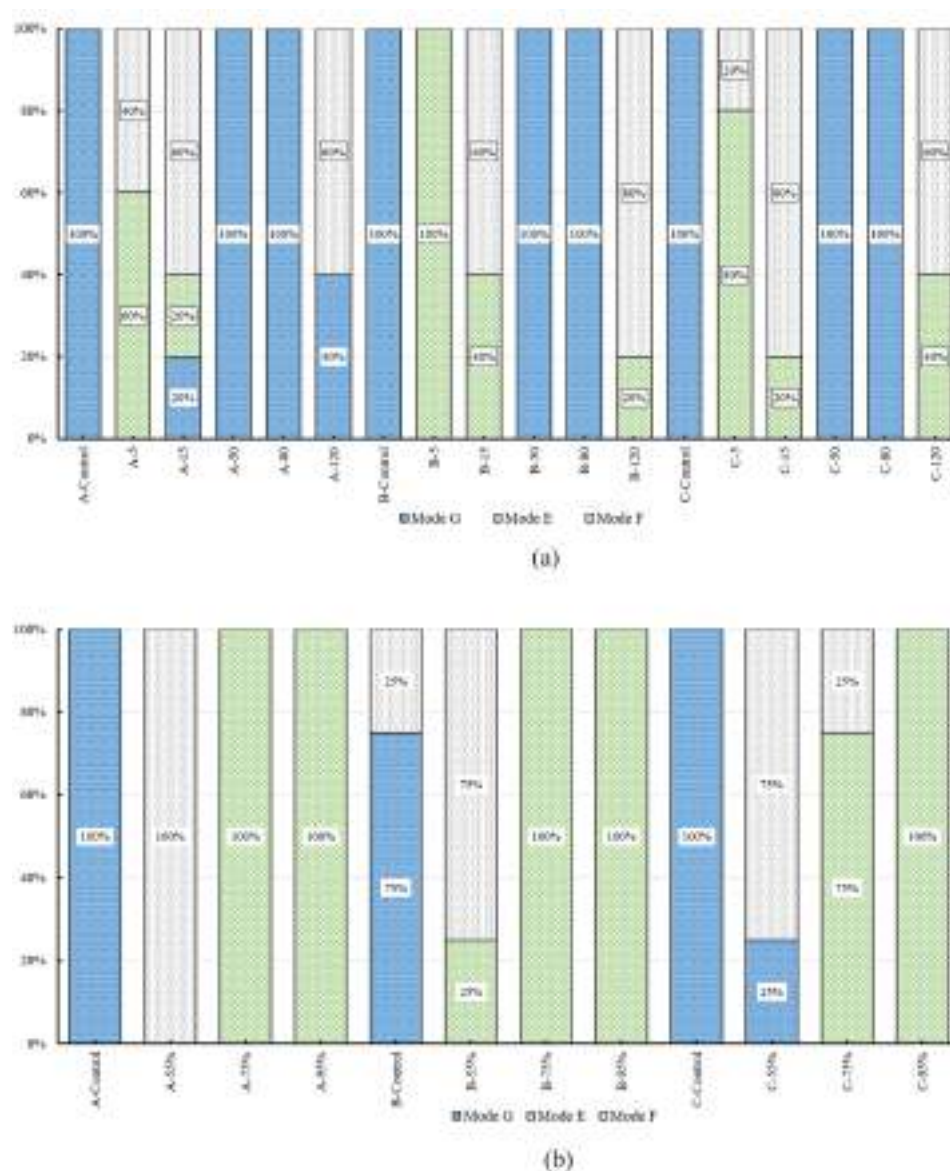
Upon increasing the surface temperature beyond 50°C, a significant loss in pull-off strength was observed due to thermal degradation or oxidative cross-linking.

A clear decrease of the pull-off adhesion for the specimens with high moisture content surface can be observed. Compared with the control specimen in group A, decreases of 20.07% and 25.84% were observed for 55% and 75% moisture content, respectively. A similar trend was held for groups B and C. In addition, the results indicate that group B showed generally lower bond strength.

### 3.5.2 | Twist-off test

The results of twist-off bond strength can also be seen in Tables 5 and 6. The percentage of change compared with

**FIGURE 11** Fraction of failure mode of the pull-off test: (a) effect of temperature and b) effect of surface moisture content



control samples are presented in Table 8. The bond strengths of control specimens from groups A, B, and C were 9.88, 8.89, and 9.11 MPa, respectively. According to the findings in the twist-off tests, the decrease in mortar specimens surface temperature and curing temperature of epoxy from room temperature leads to reduction of the bond between epoxy and mortar.

According to Table 6, the presence of moisture at the epoxy–mortar substrate interface reduced the adhesion strength. As shown in Table 8, the percentage decrease depends on the compressive strength of the substrate. Figure 13 shows the effect of pre-temperature and moisture content of the substrate before applying FRP over mortar block on the pull-off and twist-off strength. The vertical lines represent the standard deviations of the pull-off and twist-off strengths. In general, the twist-off test showed a similar trend as the pull-off test,

(Figure 14). These findings are consistent with previous reports.<sup>61</sup>

### 3.6 | Statistical analysis

In order to better understand the impact of various factors (independent variables) and their interactions on the responses (dependent variables), observed data for bond strength was analyzed using SPSS using the ANOVA. This analysis was undertaken for differences at 0.05 significance level.

Significant differences were calculated utilizing the post hoc test of Tukey and Dunnett T3, depending on the homogeneity of variances and Levene's test results. Table 9 shows the results of the ANOVA for pull-off and twist-off bond strength. The temperature, surface

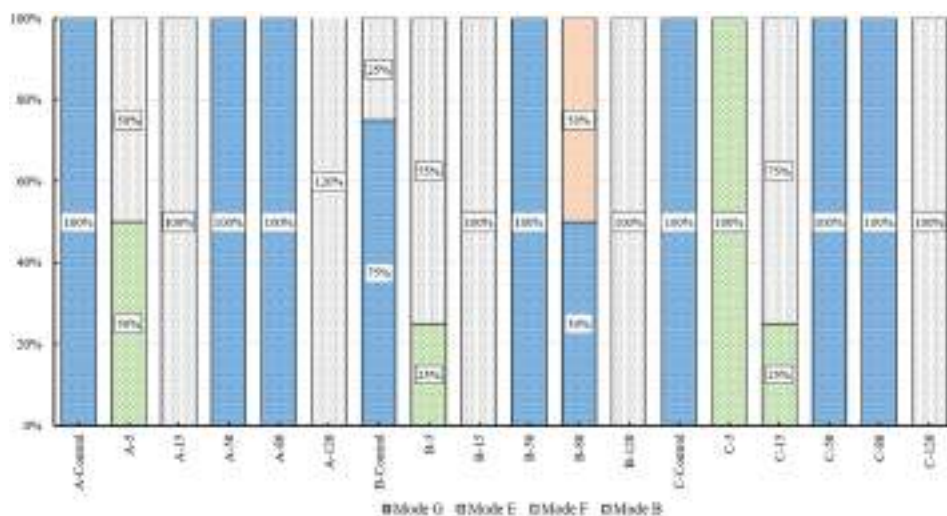


FIGURE 12 Fraction of failure mode of the twist-off test: (a) effect of temperature and (b) effect of surface moisture content

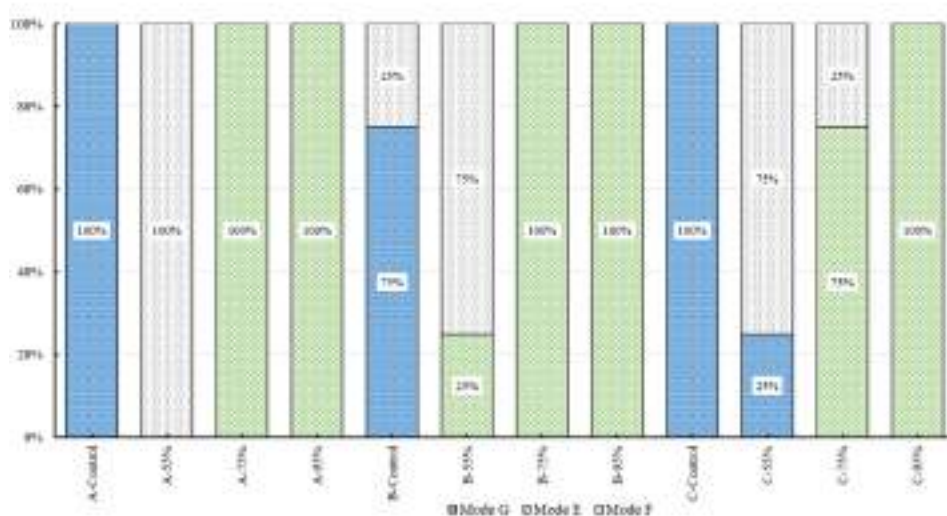


TABLE 7 Percentage of change compared with control samples on the pull-off test

Group	Percentage of change compared with control samples (%)							
	5°C	15°C	50°C	80°C	120°C	55%SMC	75%SMC	95%SMC
A	-14.04	-7.31	25.63	1.66	-12.71	-20.07	-25.84	-80.35
B	-15.62	-6.90	11.94	-3.06	-21.00	-35.48	-44.20	-100
C	-27.10	-25.03	17.75	-3.14	-7.50	-23.80	-33.15	-94.01

TABLE 8 Percentage of change compared with control samples on the twist-off test

Group	Percentage of change compared with control samples (%)							
	5°C	15°C	50°C	80°C	120°C	55%SMC	75%SMC	95%SMC
A	-18.37	-25.22	9.99	-15.25	-36.07	-17.66	-42.04	-76.37
B	-26.27	-4.36	10.44	-6.13	-29.45	-11.36	-40.76	-100
C	-5.71	-4.72	11.23	-1.92	-30.26	-12.58	-39.65	-74.90



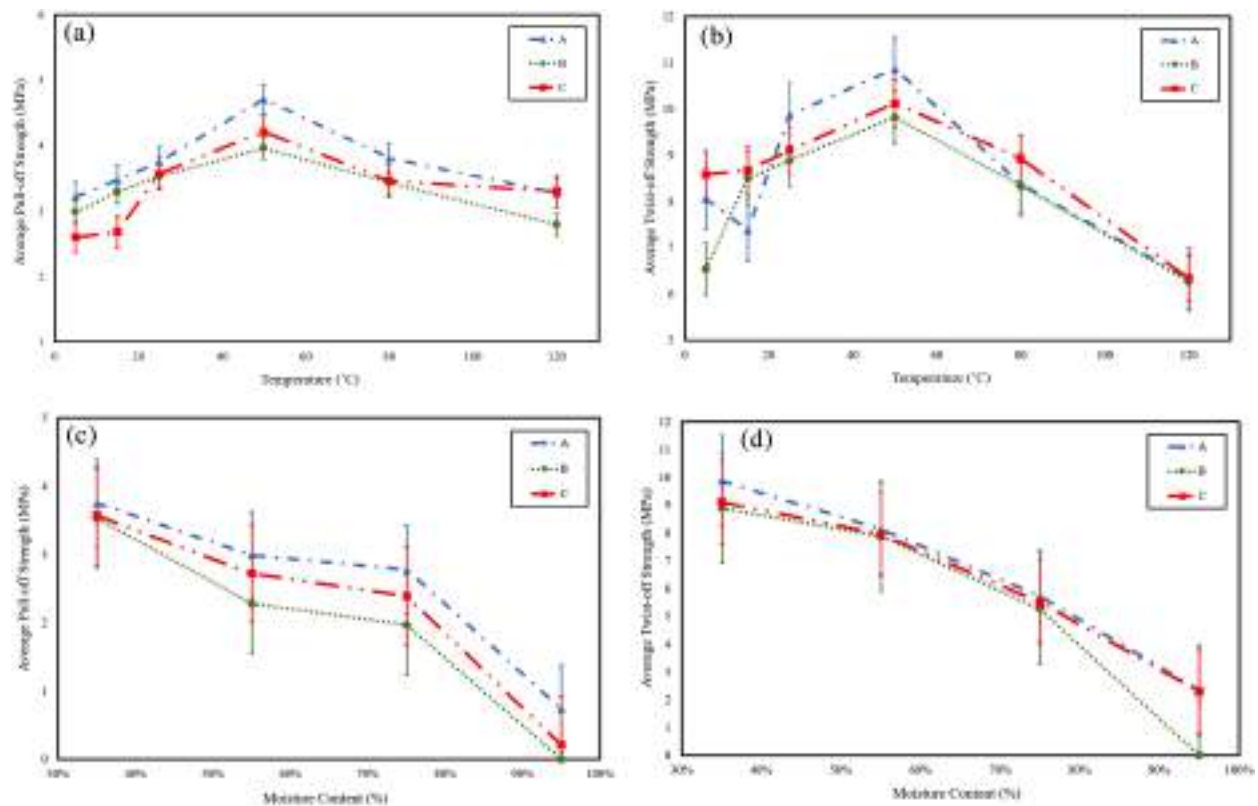


FIGURE 13 Average values of bond strength: (a) pull-off at different temperature, (b) twist-off at different temperature, (c) pull-off at different moisture content, and (d) twist-off at different moisture content

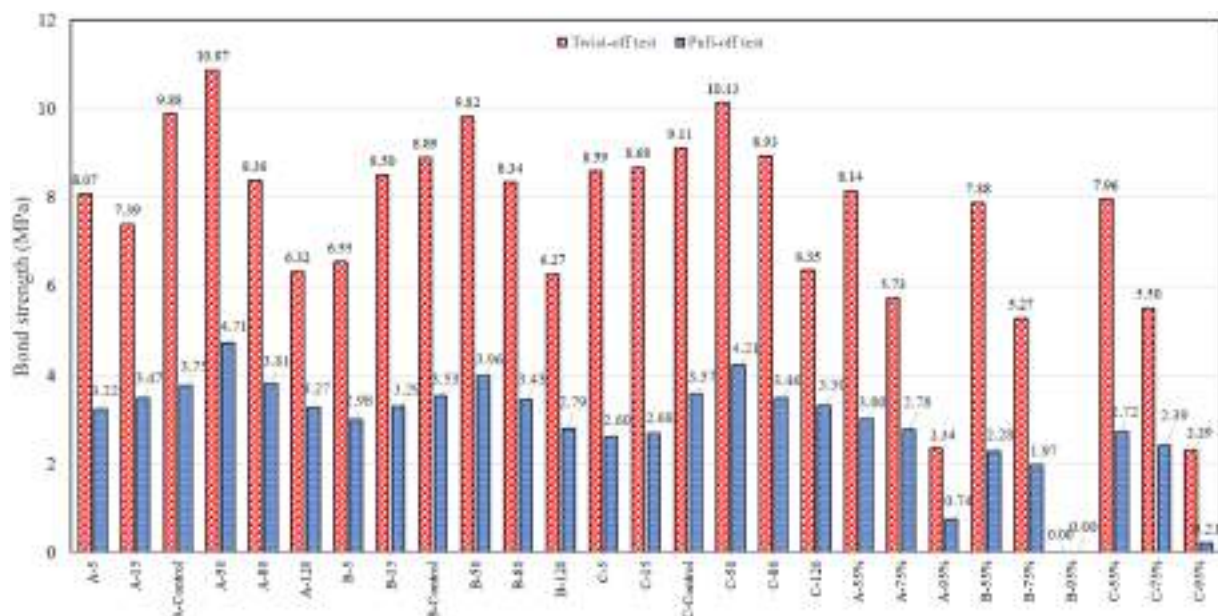


FIGURE 14 Comparison of bond strength pull-off and twist-off

moisture contents, mortar compressive strength, total porosity, and their interactions were considered as controllable factors, although the dependent variables were pull-off and twist-off bond strength.

As it can be seen, in Table 9, all factors significantly affecting pull-off and twist-off strength, except compressive strength ( $F_c$ ) and porosity ( $\phi$ ), where the significance of the  $p$ -value is more than 0.05.



TABLE 9 ANOVA results for pull-off and twist-off strength

	Sums of squares		Df	Mean squares		p-value	
Factor	Pull-off	Twist-off		Pull-off	Twist-off	Pull-off	Twist-off
Manner effects							
<i>T</i> : Temperature	63.043	219.594	5	12.609	43.919	0.000	0.000
<i>R</i> : Surface moisture content	139.513	544.845	6	23.252	90.808	0.000	0.000
<i>F</i> <sub>c</sub> : Compressive Strength	2.292	9.958	2	3.145	4.979	0.089	0.493
<i>ϕ</i> : Porosity	2.292	9.958	2	3.145	4.979	0.089	0.493
Interactions							
<i>TRF</i> <sub>c</sub> <i>ϕ</i>	159.893	724.574	26	6.150	27.868	0.000	0.000

The post hoc results showed significance of the differences between the average values of control and higher temperatures (50 and 80°C) in both pull-off and twist-off tests. Although installation of GFRP laminates at temperatures below 25°C reduced the bond strength, this reduction was not significant, especially in the twist-off test. Turkey post hoc analysis revealed that surface moisture content induced clear changes in pull-off strength at 55 ( $p = 0.000$ ), 75 ( $p = 0.000$ ), and 95 ( $p = 0.000$ ), compared with 35%. However, in twist-off strength, correlations between surface moisture content of control and values of 55%, 75%, and 95% represent  $p$  values of greater than 0.05, equal to 0.000, and equal to 0.000, respectively. The results also indicated that the mean score, of compressive strength and porosity, for the three groups mortar was not significantly different with each other.

#### 4 | PROPOSED BOND STRENGTH MODELS

The proposed new bond strength models for pull-off and twist-off tests are based on 135 and 108 experimental tests results, respectively. The proposition is based on the expected or observed behavior of experimental tests. For example, when the surface moisture content increases, adhesion strength decreased. Another expected behavior is that there must be a direct relation between compressive strength and porosity of cementitious substrate and the FRP laminate strength. Having such considerations in mind, and due to the lack and unavailability of a relation between bond strength and environmental conditions at the time being, several different types of general models were considered for pull-off and twist-off tests. The findings of regression analysis showed the most accurate equations for pull-off and twist-off bond strength expressed as follows:

$$f_p = 0.144F_c^{0.702} \times (2 - 4.623T^{-0.263} \times R^{2.918}) \quad (5)$$

$$f_T = 2.213F_c^{0.377} \times (1 - 1.851T^{-0.22} \times R^{3.667}) \quad (6)$$

In the proposed models, independent parameters  $F_c$ ,  $T$ , and  $R$  are compressive strength of substrate, surface temperature, and surface moisture content of substrate, respectively. Also,  $f_p$  and  $f_T$  are pull-off and twist-off strengths, respectively. According to statistical study and findings, since the total porosity displayed the same effects as compressive strength of cement-based mortar, the latter was considered in the proposed models. The unknown coefficients for these models are computed using nonlinear regression to provide the most accurate predictions. Four different error estimators of  $R^2$ , root mean square error (RSME), mean absolute error (MAE), and integral absolute error (IAE) were considered and calculated. The values of  $R^2$ , RSME, MAE, and IAE for pull-off model were 0.971, 0.404, 0.202, and 0.136, respectively. The values of  $R^2$ , RSME, MAE, and IAE for twist-off model were 0.970, 0.224, 0.198, and 0.179, respectively.

It should be noted that a lower value of RMSE, MAE, and IAE indicates a higher accuracy of a relation. However, the range of  $R^2$  is from 0 to 1 and the values closer to 1 show a better fit for a model.

Also presented, in Figure 15, is a logarithmic trend line that correlates the values obtained with the twist-off test with the corresponding values measured with the pull-off test.

#### 5 | SUMMARY AND CONCLUSIONS

Mechanical bond strength tests were conducted on cement-based mortar substrate and GFRP laminate

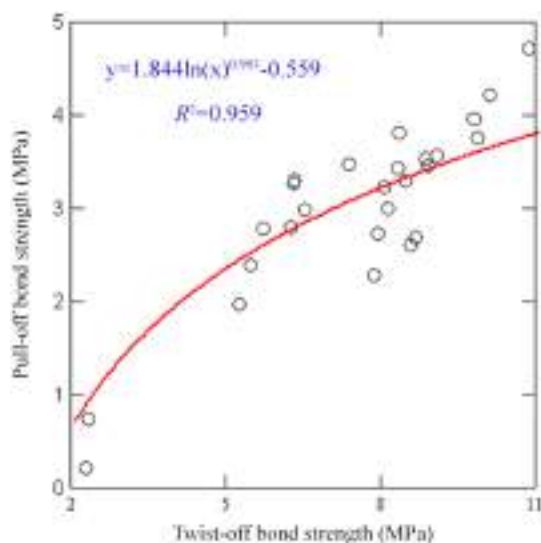


FIGURE 15 Correlation between twist-off test and pull-off test results

installed using wet layup techniques to assess the effects of environmental conditions during the installation process on the quality and performance of the bond. The bond strengths between GFRP and mortar substrate were obtained using pull-off and twist-off tests, which indicate two different modes of fracture I and fracture II, respectively. The significant findings of this study can be summarized as follows:

- Depending on the environmental conditions of the substrate, four different failure modes were observed as follows: cohesive failure in mortar substrate, cohesive failure in FRP, adhesive failure at the interface between GFRP and mortar substrate, and mixed-mode failure including mortar failure and interface failure.
- In general, the failure mode was initially cohesive within the mortar substrate for temperature range of 25–80°C. Whereas for temperature from 15 to 5°C failure modes were mixed or interface failure. Additionally, increasing the temperature beyond  $T_g$  of the adhesive, cohesive mode of failure (failure within the mortar substrate) changes to mixed or interfacial failure between adhesive and substrate.
- Test results revealed that the high surface moisture content causes a substantial decrease in the adhesive bond strength between GFRP and cementitious mortar substrate. Under these conditions, the presence of a thin layer of water on the interface is detrimental to have a proper epoxy–substrate bond. As a result, the failure mode shifted to interfacial failure with increasing surface moisture content indicating loss of adhesion.
- The percentage of occurred mixed failure mode for twist-off was more than pull-off test.

- The pull-off bond strength of A-50, B-50, and C-50 increased by 25.63%, 11.94%, and 17.75%, respectively, while the percentage of increase of twist-off bond strength was 9.99, 10.44, and 11.23. This is probably because of an increase of the cross-linking with increasing curing temperature,  $T_g$ , and a decrease in the free volume in the adhesive microstructure.
- For specimens strengthened at higher temperature than  $T_g$ , temperature has a negative effect on the bond performance and properties of epoxy resin. Furthermore, the pull-off adhesive strength reduced to 3.27, 2.79, and 3.30 MPa. Based on twist-off test results, adhesive strengths were reduced by 29%–36% in comparison to the control specimens. In this case, because the curing temperature was higher than the  $T_g$ , the network degradation can occur and with it comes degradation of mechanical properties of adhesive.
- High surface moisture content of substrate induces a progressive and significant decrease in the bond strengths of the GFRP–mortar systems investigated.
- The pull-off strength was reduced by 25.84%, 44.2%, and 33.15% when 75% surface moisture content is present. The results also revealed that adhesive bond was severely affected by surface moisture content of 95% in which failure occurred without any significant external provocation.
- Analysis of variance showed that surface temperature and moisture content had great influence on pull-off and twist-off strength, where the significance of the  $p$ -value was  $<0.05$ . The results confirmed that no statistically significant difference existed between compressive strength and porosity with the bond strength tests. The four-way ANOVA results showed the interaction of  $T$ ,  $R$ ,  $F_c$ , and  $\phi$  has a significant effect on adhesive strength.
- New and very accurate models were proposed for calculating pull-off and twist-off strength ( $f_p$  and  $f_T$ ) based on outcomes of nonlinear regression on the set of experimental data recorded and significant parameter of temperature, moisture content, and compressive strength ( $T$ ,  $R$ , and  $F_c$ ).
- A logarithmic trend line was fitted very well to the data of pull-off and twist-off tests conducted in this study.

$$f_p = 1.8 \ln(f_T) - 0.6$$

## ACKNOWLEDGMENTS

The authors would like to express their gratitude to the department of civil engineering at Ferdowsi University of Mashhad for their support. They also appreciate the help

provided by staff of structural laboratory at Ferdowsi University of Mashhad and research and development laboratory at Par-e-Tavous Research Institute.


## CONFLICT OF INTEREST

The authors declare that they have no conflict of interest that may affect their judgment or influence the outcome of this research.

## DATA AVAILABILITY STATEMENT

The data that support the findings of this study are available from the corresponding author upon reasonable request.

## ORCID

Mohammadreza Tavakkolizadeh  <https://orcid.org/0000-0002-0932-4605>

## REFERENCES

- Kanareh HM. Concrete floors and moisture. Skokie, IL: National Ready Mixed Concrete Association, Engineering Bulletin 119, Portland Cement Association; 2005.
- Myers J, Ekenel M. Effect of environmental conditions on bond strength between CFRP laminate and concrete substrate. Special Publication. 2005;230:1571–92.
- Sika Group. Solutions/product datasheets. Switzerland. 2012. Available from: <http://www.sika.com>.
- Wan B, Petrou MF, Harries KA. The effect of the presence of water on the durability of bond between CFRP and concrete. J Reinf Plast Compos. 2006;25(8):875–90.
- Dai J-G, Yokota H, Iwanami M, Kato E. Experimental investigation of the influence of moisture on the bond behavior of FRP to concrete interfaces. J Compos Construct. 2010;14(6): 834–44.
- Lu Y, Zhu T, Li S, Liu Z. Bond behavior of wet-bonded carbon fiber-reinforced polymer-concrete interface subjected to moisture. Int J Polym Sci. 2018;2018:1–11.
- Cuomo M, Caponetto R, Presti AL, Ardizzone E. Experimental evaluation of the effect of partial saturation of construction moisture on CFRP-concrete debonding. Compos Part B Eng. 2017;127:70–7.
- Pan Y, Shi J, Xian G. Experimental and numerical study of the CFRP-to-concrete bonded joints after water immersion. Compos Struct. 2019;218:95–106.
- Pan Y, Xian G, Silva MA. Effects of water immersion on the bond behavior between CFRP plates and concrete substrate. Construct Build Mater. 2015;101:326–37.
- Shrestha J, Zhang D, Ueda T. Durability performances of carbon fiber-reinforced polymer and concrete-bonded systems under moisture conditions. J Compos Construct. 2016;20(5): 04016023.
- Ouyang Z, Wan WB. Experimental and numerical study of water effect on bond fracture energy between FRP and concrete in moist environments. J Reinf Plast Compos. 2008;27(2):205–23.
- Ouyang Z, Wan B. Nonlinear deterioration model for bond interfacial fracture energy of FRP-concrete joints in moist environments. J Compos Construct. 2009;13(1):53–63.
- Mays GC, Hutchinson AR. Adhesives in civil engineering. Cambridge, England: Cambridge University Press; 1992.
- ACI Committee. 440. Guide for the design and construction of externally bonded FRP Systems for Strengthening Concrete Structures (ACI.440.2R-17). Farmington Hills, MI: American Concrete Institute; 2017.
- AASHTO-FRPS-1. Guide specifications for design of bonded FRP systems for repair and strengthening of concrete bridge elements. Washington, DC: American Association of State Highway and Transportation Officials; 2010.
- Bulletin No. 14, Externally bonded FRP reinforcement for RC structures. Technical report. International Federation for Structural Concrete (fib), Lausanne, Switzerland, 2001.
- Aiello M, Frigione M, Acierno D. Effects of environmental conditions on performance of polymeric adhesives for restoration of concrete structures. J Mater Civil Eng. 2002;14(2):185–9.
- Borchert K, Zilch K. Bond behaviour of NSM FRP strips in service. Struct Concrete. 2008;9(3):127–42.
- Luo S, Wong CP. Thermo-mechanical properties of epoxy formulations with low glass transition temperatures. Proceedings of the 8th International Symposium on Advanced Packaging Materials. 2002; 226–231.
- Xian G, Karbhari VM. Segmental relaxation of water-aged ambient cured epoxy. J Polym Degrad Stab. 2007;92(9):1650–9.
- Ferrier E, Rabinovitch O, Michel L. Mechanical behavior of concrete-resin/adhesive-FRP structural assemblies under low and high temperatures. Construct Build Mater. 2015;127: 1017–28.
- Nguyen T, Bai Y, Zhao X, Al-Mahaidi R. Mechanical characterization of steel/CFRP double strap joints at elevated temperature. Compos Struct. 2011;93(6):1604–12.
- Leone M, Matthys S, Aiello MA. Effect of elevated service temperature on bond between FRP EBR systems and concrete. Compos B. 2009;40(1):85–93.
- Blontrock H, Taerwe L, Vanwalleghem H. Bond testing of externally glued FRP laminates at elevated temperature, the international conference on bond in concrete—from research to standard, Budapest, Hungary; 2002.
- Attari B, Tavakkolizadeh M. An experimental investigation on effect of elevated temperatures on bond strength between externally bonded CFRP and concrete. Steel Compos Struct. 2019; 32(5):559–69.
- Al-Shawaf A, Al-Mahaidi R, Zhao X. Study on bond characteristics of CFRP/steel double lap shear joints at subzero temperature exposure. 3rd International Conference on FRP Composites in Civil Engineering (CICE), Miami, FL; 2006.
- Kim Y, Hossain M, Yoshitake I. Cold region durability of a two-part epoxy adhesive in double-lap shear joints: experiment and model development. J Construct Build Mater. 2012;36: 295–304.
- ASTM Standard C109-20. Standard test method for compressive strength of hydraulic cement mortars. West Conshohocken, PA (2020).
- ASTM Standard C144-18. Standard specification for concrete aggregates. West Conshohocken, PA; 2018.
- ASTM Standard C128-15. Standard test method for relative density and absorption of fine aggregate. West Conshohocken, PA: ASTM International; 2015.
- Abo Sabah SH, Zainal NL, Muhamad Bunnori N, Megat Johari MA, Hassan MH. Interfacial behavior between normal

- substrate and green ultra-high-performance fiber-reinforced concrete under elevated temperatures. *Struct Concrete*. 2019; 20:1869–908.
32. Courard L, Piotrowski T, Garbacz A. Near-to-surface properties affecting bond strength in concrete repair. *Cement Concrete Compos*. 2014;46:73–80.
  33. Sabzi J, Esfahani MR. Effects of tensile steel bars arrangement on concrete cover separation of RC beams strengthened by CFRP sheets. *Construct Build Mater*. 2018;162:470–9.
  34. Saljoughian A, Mostofinejad D. Using grooving and corner strip-batten techniques for seismic strengthening of square reinforced concrete columns with fiber-reinforced polymer composites. *Struct Concrete*. 2020;21(5):2066–82.
  35. ASTM Standard C230-20. Standard specification for flow table for use in tests of hydraulic cement. West Conshohocken, PA; 2020.
  36. ASTM Standard C1403-15. Standard test method for rate of water absorption of masonry mortars. West Conshohocken, PA; 2015.
  37. ASTM Standard C642-13. Standard test method for density, absorption, and voids in hardened concrete. West Conshohocken, PA; 2013.
  38. ASTM Standard D4541-17. Standard test method for pull-off strength of coatings using portable adhesion testers. West Conshohocken, PA; 2017.
  39. ASTM Standard D7522-15. Standard test method for pull-off strength for FRP laminate systems bonded to concrete substrate. West Conshohocken, PA; 2015.
  40. ASTM Standard D7234-19. Standard test method for pull-off adhesion strength of coatings on concrete using portable pull-off adhesion testers. West Conshohocken, PA; 2019.
  41. BS EN 1542. Products and systems for the protection and repair of concrete structures. Test methods Measurement of bond strength by pull-off British Standard Institution; 1999.
  42. BS 1881-207. Recommendations for the assessment of concrete strength by near-to-surface tests. British Standard Institutions; 1992.
  43. CNR-DT 200. Guide for the design and construction of externally bonded FRP systems for strengthening existing structures. Italy: National Research Council; 2004.
  44. Cleland D, Long AE. The pull-off test for concrete patch repairs. *Proc Inst Civil Eng—Struct Build*. 1997;122(4): 451–60.
  45. Bungey J, Madandoust R. Factors influencing pull-off tests on concrete. *Magaz Concr Res*. 1992;44(158):21–30.
  46. Moczulski G, Garbacz A & Courard L Evaluation of the effect of load eccentricity on pull-off strength. *Concrete Repair, Rehabilitation and Retrofitting II*; 2009:pp. 367–368.
  47. Bonaldo E, Barros JA, Lourenço PB. Bond characterization between concrete substrate and repairing SFRC using pull-off testing. *Int J Adhes Adhes*. 2005;25(6):463–74.
  48. Eveslage T, Aidoo J, Harries KA, Bro W. Effect of variations in practice of ASTM D7522 standard pull-off test for FRP-concrete interfaces. *J Test Evaluat*. 2010;38(4):424–30.
  49. Naderi M. New twist-off method for the evaluation of in-situ strength of concrete. *J Test Evaluat*. 2007;35(6):602–8.
  50. ChRndaprasirt P, Buapa N, Cao H. Mixed cement containing fly ash for masonry and plastering work. *Construct Build Mater*. 2005;19(8):612–8.
  51. Bullard JW. Virtual cement and concrete testing laboratory version 9.5 user guide NIST Special Publication 1173; 2014.
  52. Watts BE, Tao C, Ferraro CC, Masters FJ. Proficiency analysis of VCCTL results for heat of hydration and mortar cube strength. *J Constr Build Mater*. 2018;161:606–17.
  53. Bullard JW, Stutzman PE, Ordoñez Belloc LM, Garboczi EJ, Bentz DP. Virtual cement and concrete testing laboratory for quality testing and sustainability of concrete. *ACI Special Publication SP-266*; 2009, pp. 27–36.
  54. Bentz DP. Modeling the influence of limestone filler on cement hydration using CEMHYD3D. *J Cem Concr Compos*. 2006;28: 124–9.
  55. Watts BE, Ferraro CC. Prediction of setting for admixture modified mortars using the VCCTL. *J Cem Concr Compos*. 2017;78: 63–72.
  56. Kim Y-Y, Lee K-M, Bang J-W, Kwon S-J. Effect of w/c ratio on durability and porosity in cement mortar with constant cement amount. *Adv Mater Sci Eng*. 2014;2014:1–11.
  57. Shrestha J, Ueda T, Zhang D. Durability of FRP concrete bonds and its constituent properties under the influence of moisture conditions. *J Mater Civil Eng*. 2015;27(2):A4014009.
  58. Kinloch AJ. Adhesion and adhesives: science and technology. Berlin, Germany: Springer Science & Business Media; 2012.
  59. Campana C, Leger R, Sonnier R, Ferry L, Ienny P. Effect of post curing temperature on mechanical properties of a flax fiber reinforced epoxy composite. *Compos A: Appl Sci Manuf*. 2018;107:171–9.
  60. Carbas RJC, Marques EAS, Da Silva LFM, Lopes AM. Effect of cure temperature on the glass transition temperature and mechanical properties of epoxy adhesives. *J Adhesion*. 2014;90:104–19.
  61. Ekenel M, Myers J, Khataukar A. Affect of environmental conditions during installation process on bond strength between CFRP laminate and concrete substrate. 3rd international conference composites in construction, Lyon, France; 2005.

## AUTHOR BIOGRAPHIES



**Peyman Imani Jajarmi**, PhD Candidate, Department of Civil Engineering, Ferdowsi University of Mashhad, Azadi Square, Mashhad, Khorasan Razavi 91775-1111, Iran. Email: peyman.imani@mail.um.ac.ir



**Mohammadreza Tavakkolizadeh**, Assistant Professor, Department of Civil Engineering, Ferdowsi University of Mashhad, Azadi Square, Mashhad, Khorasan Razavi 91775-1111, Iran. Email: drt@um.ac.ir



**Abbas Youssefi**, Director, Par-e-Tavous Research Institute, Sento Highway, Mashhad, Khorasan Razavi 91375-5395, Iran. Email: ayo799@gmail.com

**How to cite this article:** Imani Jajarmi P, Tavakkolizadeh M, Youssefi A. Effect of temperature and moisture on the bond strength between fiber reinforced polymer laminates and cement-based mortar substrates. *Structural Concrete*. 2022;23:970–92. <https://doi.org/10.1002/suco.202100490>